Monitoring thermally-induced phase transitions in porcine cornea with the use of fluorescence micro-imaging analysis

F. Rossi[1], P. Matteini[1,2], I. Bruno[3], P. Nesi[3], R. Pini[1]*

[1]*Istituto di Fisica Applicata "Nello Carrara", Consiglio Nazionale delle Ricerche, Firenze, Italy*
[2]*Dipartimento di Chimica Organica "Ugo Schiff ", Università di Firenze, Firenze, Italy*
[3]*Dipartimento di Sistemi e Informatica, Università di Firenze, Firenze, Italy*
**Contact author: r.pini@ifac.cnr.it*

Abstract: Thermal modifications induced in corneal stroma were investigated with the use of fluorescence microscopy. Tissue samples were heated in a water bath at temperatures in the 35-90°C range. Fluorescence images of the structural modifications induced were acquired after staining with Indocyanine Green (ICG). Discrete Fourier Transform (DFT) and entropy analyses of each image made it possible to characterize the thermally-induced phase transitions in the stroma, and to indicate a threshold value for high thermal damage. The procedure could be proposed as the basis for a real-time controlling system for surgical techniques based on induced thermal effects.

OCIS codes: (100.2960) Image analysis; (120.6810) Thermal effects; (170.2520) Fluorescence microscopy

References and links

1. R. Brinkmann, N. Koop, G. Geerling, J. Kampmeier, S. Borcherding, K. Kamm, R. Birngruber, "Diode laser thermokeratoplasty: application strategy and dosimetry," J. Cataract Refract. Surg. **24**,1195–207 (1998).
2. F. Rossi, R. Pini, L. Menabuoni, R. Mencucci, U. Menchini, S. Ambrosini, G. Vannelli, "Experimental study on the healing process following laser welding of the cornea," J. Biomed. Opt. **10**, 024004 (2005).
3. K. Suthamjariya, R. Rox Anderson, "Laser in Dermatology," in *Biomedical Photonics Handbook*, T. Vo-Dinh, Ed., (CRC Press 2003), pp. 40/1-40/40.
4. A.L. Wallace, R.M. Hollinshead, C.B. Franck, "The scientific basis of thermal capsular shrinkage," J. Shoulder Elbow Surg. **9**, 354-360 (2000).
5. J. Kampmeier, B. Radt, R. Birngruber, R. Brinkmann, "Thermal and biomechanical parameters of porcine cornea," Cornea **19**, 355-363 (2000).
6. C.A. Miles, T.V. Burjanadze, A.J. Bailey, "The kinetics of the thermal denaturation of collagen in unrestrained rat tail tendon determined by differential scanning calorimetry," J. Mol. Biol. **245**, 437-446 (1995).
7. F. Flandin, C. Buffevant, D. Herbage, "A differential scanning calorimetry analysis of the age-related changes in the thermal stability of rat skin collagen," Biochim. Biophys. Acta **791**, 205-211 (1984).
8. P. Kronick, B. Maleeff, and R. Carroll, "The locations of collagens with different thermal stabilities in fibrils of bovine reticular dermis," Connect. Tissue Res. **18**, 123-134 (1988).
9. R. Agah, J.A. Pearce, A.J. Welch, and M. Motamedi, "Rate process model for arterial tissue thermal damage: implications on vessel photocoagulation," Lasers Surg. Med. **15**, 176-184 (1994).
10. A.D. Zweig, B. Meierhofer, O.M. Muller, C. Mischler, V. Romano, M. Frenz, and H.P. Weber, "Lateral thermal damage along pulsed laser incisions," Lasers Surg. Med. **10**, 262-274 (1990).
11. T. Tanaka, S. Furutani-Miura, M. Nakamura, and T. Nishida, "Immunohistochemical study of localization of extracellular matrix after holmium YAG laser irradiation in rat cornea," Jpn. J. Ophthalmol. **44**, 482-488 (2000).
12. S.J. Lin, C.Y. Hsiao, Y. Sun, W. Lo, W.C. Lin, G.J. Jan, S.H. Jee, C.Y. Dong, "Monitoring the thermally induced structural transitions of collagen by use of second-harmonic generation microscopy," Opt. Lett. **30**, 622-624 (2005).
13. T. Theodossiou, G.S. Rapti, V. Hovhannisyan, E. Georgiou, K. Politopoulos, D. Yova, "Thermally induced irreversible conformational changes in collagen probed by optical second harmonic generation and laser-induced fluorescence," Lasers Med. Sci. **17**, 34-41 (2002).
14. M.G. Lin, T.L. Yang, C.T. Chiang, H.C. Kao, J.N. Lee, W. Lo, S.H. Jee, Y.F. Chen, C.Y. Dong, S.J. Lin, "Evaluation of dermal thermal damage by multiphoton autofluorescence and second-harmonic-generation microscopy," J. Biomed. Opt. **11**, 064006 (2006).

#83788 - $15.00 USD Received 4 Jun 2007; revised 25 Jul 2007; accepted 25 Jul 2007; published 21 Aug 2007

15. G. Cox, E. Kable, A. Jones, I. Fraser, F. Manconi, and M.D. Gorrell, "3-dimensional imaging of collagen using second harmonic generation," J. Struct. Biol. **141**, 53-62 (2003).
16. H. Y. Tan, S. W. Teng, W. Lo, W. C. Lin, S. J. Lin, S. H. Jee, C. Y. Dong, "Characterizing the thermally induced structural changes to intact porcine eye, part 1: second harmonic generation imaging of cornea stroma," J. Biomed. Opt. **10**, 054019 (2005).
17. G. Wollensak, E. Spoerl, T. Seiler, "Stress-strain measurements of human and porcine corneas after riboflavin–ultraviolet-A-induced cross-linking," J. Cataract Refract. Surg. **29**, 1780–1785 (2003)
18. M.L.J. Landsman, G. Kwant, G. A. Mook, W. G. Zijlstra, "Light- absorbing properties, stability, and spectral stabilization of indocyanine green," J. Appl. Physiol. **40**, 575-583 (1976).
19. L.-P. Kamolza, H. Andel , W. Haslik , A. Donner , W. Winter , G. Meissl , M. Frey, "Indocyanine green video angiographies help to identify burns requiring operation," Burns **29**, 785–791 (2003).
20. L. A. Yannuzzi, M. D. Ober, J. S. Slakter, R. F. Spaide, Y L. Fisher, R.W. Flower, R. Rosen, "Ophthalmic fundus imaging: today and beyond," Am. J. Ophthalmol. **137**, 511-524 (2004).
21. G.P. Holley, A.Alam, A. Kiri, H.F. Edelhauser, "Effect of indocyanine green intraocular stain on human and rabbit corneal endothelial structure and viability. An in vitro study," J. Cataract Refract. Surg. **28**, 1027-1033 (2002).
22. T. John, "Use of indocyanine green in deep lamellar endothelial keratoplasty," J. Cataract Refract. Surg. **29**, 437–443 (2003).
23. L. Menabuoni, R. Pini, F. Rossi, I. Lenzetti, S. H. Yoo, J.-M. Parel, "Laser-assisted corneal welding in cataract surgery: a retrospective study," J. Cataract Refract. Surg. (to be published).
24. K.M. McNally-Heintzelman, "Laser Tissue Welding," in *Biomedical Photonics Handbook*, Vo-Dinh T ed. (CRC Press, 2003), Chap. 39, pp. 1-45.
25. A.J. Welch, M. Van Germert, *Optical-thermal response of laser-irradiated tissue* (Plenum Press, 1995).
26. A. Jain, *Fundamentals of digital image processing* (Prentice-Hall, 1989)
27. M.N. Asiyo-Vogel, R. Brinkmann, H. Notbohm, R. Eggers, H. Lubatschowski, H. Laqua, A. Vogel, "Histologic analysis of thermal effects of laser thermokeratoplasty and corneal ablation using Sirius-red polarization microscopy," J. Cataract Refract. Surg. **23**, 515-26 (1997).

1. Introduction

Thermal therapies are increasingly used in clinical practice for the treatment of diseases and injuries. Heat-induced effects have been exploited in ophthalmology for refractive surgery [1] and for the closure of corneal wounds [2]; in dermatology, for skin rejuvenation and resurfacing or for the treatment of cutaneous vascular lesions [3]; in orthopedics, for the thermal treatment of shoulder instability [4]. The heating devices employed are based principally on the use of laser irradiation, radiofrequency electrical current, or microwaves. The main problem to solve, independently of applications and devices, is the control of the heating effect induced, during both the surgical treatment and the healing. In fact, monitoring thermally-induced structural modifications in connective tissues is of utmost importance in verifying the efficacy of the procedure and in preventing undesirable thermal damage to the surrounding tissues.

Structural changes in connective tissue resulting from therapeutic thermal treatments are primarily imputable to fibrillar collagen, the most common type of collagen in these tissues. This protein has a crystalline triple-helical tertiary structure that is transformed into an amorphous random coil configuration upon heating. Several techniques have been employed to characterize thermal modifications of collagen tissue. Calorimetric studies have typically been conducted using Differential Scanning Calorimetry (DSC). This method makes it possible to characterize the thermodynamic behavior of many connective tissues, which then show substantial improvement compared to the use of other previously-adopted approaches [5-8]. On the other hand, histological techniques (e.g. histological staining and immuno-fluorescent labeling) remain the most commonly-used imaging platform, due to their relative ease of use [9-11]. Transmission Electron Microscopy (TEM) is used when high resolution is required [9, 11], but it involves high costs as well as complex protocols for specimen processing. Although DSC and the afore-mentioned microscopy techniques may be very useful when used on tissue *ex vivo*, they are unsuitable for monitoring heat-induced changes *in vivo*. Recently, Second Harmonic Generation (SHG) microscopy has been proposed as an alternative approach, as it is capable of furnishing accurate thermal responses without the need for histological or labeling protocols [12-14]. Furthermore, this technique has the potential to be developed into an effective imaging tool for *in vivo* characterization. However, two main

#83788 - $15.00 USD Received 4 Jun 2007; revised 25 Jul 2007; accepted 25 Jul 2007; published 21 Aug 2007

factors of SHG make the technique intrinsically unsuitable for tissue phase-transition characterization: firstly, the analysis has to be limited to fibrillar collagen, as it is the only component possessing nonlinear optical properties [15]; secondly, the signal rapidly decreases with an increase in the temperature, and is therefore ineffective in accurately detecting changes beyond the main peak of collagen denaturation [14].

In this paper we present an imaging system for monitoring thermally-induced phase transitions in connective tissues. The procedure is based on the use of fluorescence micro-imaging analysis of ICG-stained tissues. Our study was performed on porcine corneas, because this kind of connective tissue has a very regular structure and its thermal and biomechanical parameters are well-known [5, 16, 17]. Corneal collagen is regularly arranged in fibers that are organized into lamellae, i.e. in planes running parallel to the corneal surface. ICG has the advantage of staining the tissue homogeneously and un-specifically, thus providing a bright fluorescence emission from the entire structure of the sample. ICG was chosen because its photophysical properties are well-known [18], and because of its low toxicity and use in common practice in medical diagnostics and surgery [19-22]. Specifically, it has been proposed as a photosensitizer in several applications of laser welding techniques [23, 24]. The procedure is based on a thermal process that induces immediate fusion of a wound wall. If simple analysis of the stained tissue during treatment has to be performed, it will be possible to characterize the phase transitions of the tissue. The proposed technique could thus be useful as an alternative, low-cost micro-imaging analysis for controlling thermal structural modifications in connective tissues.

2. Materials and methods

2.1. Heat bath treatment

Sixty-three freshly-enucleated, intact porcine eyes were used (mean age of the animals: 9-11 months). The entire corneas were extracted, and their transparency and integrity were controlled prior to being used in the tests. The samples were stored in BSS at room temperature for less then 6 hours. Each sample was then immersed in a water bath for five minutes. This treatment time ensured that thermal equilibrium was reached [25]. A heating immersion circulator (mod. ED, Julabo Labortechnik GmbH, Seelbach, Germany) with ±0.03 °C temperature stability and a reading error of ±0.1 °C was used to heat the water bath. The temperature values studied were in the range of interest for medical applications: namely, the values 35, 40, 45, 47, 50, 53, 55, 56, 57, 58, 59, 60, 61, 62, 63, 66, 68, 71, 74, 77, 90°C were tested. Three different corneas were heated at each temperature, in order to give statistical significance to the study. After immersion in the water bath, the samples were stored in formalin until micro-imaging was performed.

2.2. Image acquisition

Cornea samples were sliced in 200-µm-thick cross-sections, which were stained with a 0.5% (w/w) water solution of Indocyanine Green (IC-GREEN, Akorn, Buffalo Grove, IL) over a 4-minute period. The slices were briefly rinsed in water and then mounted on microscope glass slides. All measurements were performed using an inverted epifluorescence microscope (Diaphot Nikon, Tokyo, Japan) equipped with a high-pressure mercury lamp (HBO 100 W, Osram, Augsberg, Germany) as the light source. The excitation wavelengths were selected using 10-nm bandwidth interference filters (436FS10-25, Andover Corporation, Salem, NH, USA) coupled to a dichroic mirror (ND510 Diaphot Nikon). Fluorescence images were acquired using a slow-scan cooled CCD camera (Chroma CX260, DTA, Cascina, Italy) equipped with a 512x512 pixel detector (KAF261E, Kodak, Heidelberg, Germany). The thermally-induced modifications to the corneal specimens were evaluated using fluorescence images acquired with a NIR long wave pass filter (800FH90-25, Andover Corporation).

#83788 - $15.00 USD Received 4 Jun 2007; revised 25 Jul 2007; accepted 25 Jul 2007; published 21 Aug 2007

2.3. Micro-imaging analysis

Micro-imaging analysis was performed by means of two image processing techniques: the image entropy and the two-dimensional Discrete Fourier Transform (2D DFT) [26]. The entropy is a statistical index widely used in the field of information theory to express the information content of a message. It is used as a measure of redundancy in an information source. When applied to an image with a regularly repeated pattern, as the lamellar planes in a corneal stroma, a high value in image entropy means a high level in regular organization, while a low value may be related to a reduction of the number of planes visualized in the image, i.e. caused by a homogenization of the tissue. When applied in image processing, the classical entropy definition does not take into account of the spatial properties of the image. To circumvent this limitation, the 2D DFT was used to assess the geometric characteristics of the acquired image. The 2D DFT is a mathematical transformation of an image: the usual spatial domain representation is a function of two spatial variables, *f(x,y)*, indicating the intensity of the image at a particular point *(x,y)*. The Fourier transform is the frequency domain representation of an image as a sum of complex exponentials of varying magnitudes, frequencies, and phases. In the frequency domain, an edge (i.e. a line separating one region from another) is composed of a wide range of frequency components: the frequency distribution of the transformed image can be analyzed to approach the problem of finding the distribution of image lines direction and then to identify the geometry of the image textures. In particular, when considering a pattern of horizontal lines, as in the corneal stroma, the frequency distribution shape is an ellipse oriented along the orthogonal axis; in event of random patterns, instead, the distribution contains contributions due to all the directions, and the shape tends to be circular. For these reasons, the corneal stroma image spectrum was considered for further evaluation on stromal structural modifications.

Two grey levels images showing a 400x400 μm tissue area were acquired from each cornea sample, in order to visualize both the anterior and posterior corneal stroma. The two techniques were then applied, by means of a commercial software image processing tool (Matlab® 7.1, the Mathworks, Natick, MA, USA). The 2D DFT of each image was computed with the proper software function. The DFT is usually defined for a discrete function *f(m,n)* that is nonzero only over the finite region $0 \le m \le M-1$ and $0 \le n \le N-1$. The two-dimensional *MxN* DFT and inverse *MxN* DFT relationships are given by:

$$F(p,q) = \sum_{m=0}^{M-1}\sum_{n=0}^{N-1} f(m,n) e^{-j(2\pi/M)pm} e^{-j(2\pi/N)qn} \qquad \begin{matrix} p = 0,1,\ldots,M-1 \\ q = 0,1,\ldots,N-1 \end{matrix} \tag{1}$$

$$f(m,n) = \frac{1}{MN}\sum_{p=0}^{M-1}\sum_{q=0}^{N-1} F(p,q) e^{j(2\pi/M)pm} e^{j(2\pi/N)qn} \qquad \begin{matrix} m = 0,1,\ldots,M-1 \\ n = 0,1,\ldots,N-1 \end{matrix}$$

The values *F(p,q)* are the DFT coefficients of *f(m,n)*. The resulting image spectrum was then shifted so as the zero-frequency component *F(0,0)*, corresponding to the image average brightness, is displayed in the center of the frequency distribution image.

The same image source was processed by applying the *edge* function, based on Canny filter, to perform edge detection and extract the spatial distribution of the lamellar planes. The entropy was then evaluated. For an image with *L* grey levels, entropy *E* is a scalar value, defined as:

$$E = -\sum_{k=0}^{L-1} P(g_k)\log(P(g_k)) \tag{2}$$

#83788 - $15.00 USD Received 4 Jun 2007; revised 25 Jul 2007; accepted 25 Jul 2007; published 21 Aug 2007

where: $P(g_k)$ is the histogram value of the k-th grey level g_k. A new parameter was defined as the entropy inverse: it was indicated as the Disorganization Parameter (DP = 1/E), and it was used to characterize heat-induced phase transitions in the stroma.

3. Results

We acquired six fluorescence images for each temperature value. The results are shown in Fig. 1. A regular horizontal pattern of lamellar sheets was observed at temperatures in the 35° to 47°C range. At higher values (50 to 61°C), the horizontal patterns showed increasing amplitude, while undulations were evident. Above 62°C, the patterns had a random distribution in space and a considerably increasing thickness. This behavior was evidenced by the plot of the logarithm of the DFT absolute value: the DFT distribution was prevalently along the vertical axis until the temperatures were below 62°C. When a temperature of more then 63°C was induced in the tissue, the DFT distribution was uniform and the plot of its absolute value assumed a circular form. The intensity entropy was calculated for each image, and the resulting DP was plotted. The results are shown in Fig. 2, where the calculated mean DP value and the standard error of the mean are reported for each temperature. Five relative maximum peaks are present, corresponding to the temperature values of 45°C, 53°C, 57°C, ~66°C and ~75°C.

4. Discussion

Micro-imaging analysis of ICG stained corneas evidenced the thermal structural phase transitions with the use of a simple image processing procedure. The DFT spatial distribution enabled us to characterize a threshold temperature that corresponded to 63°C in the case of corneal tissue. In the 35 to 62°C range, stromal lamellae orientations were preserved, even if an increasing thickness was observed.

For temperatures above 63°C, the DFT showed a circular spatial distribution that corresponded to a randomization of the stroma organization. This temperature threshold value corresponded to the phase-transition temperature range (60 to 65°C) previously detected using a different experimental technique in corneal stroma, and was probably correlated to tissue shrinkage [27]. A discussion of the DP plot of the thermal treated cornea images is of particular interest: in the 35 to 45°C range, the cornea has a regular stromal structure, and the DP slowly increases until a first relative maximum value at 45°C is reached. Subsequent maxima are at the temperatures of 53°C, 57°C, ~66°C, and ~75°C. Above these values, the DP plot decreases. If we compare this plot with previously-published DSC and SHG plots [5, 16], it is evident that the main peaks correspond and are consistent with the principal thermal phase transitions of corneal tissue. In addition, DP technique revealed to be a more sensitive tool, since it was capable of detecting subtle changes in corneal structures. In fact, while DSC thermograms of connective tissues typically show one main peak positioned between two shoulders, DP plot evidenced five maximum transition temperature values. The major difference between the DP and the SHG approaches is that, in the latter, signal intensity decreases towards zero when high temperatures are induced in the tissue, i.e. when strong denaturation is reached [14]. This is due to the fact that the SHG signal is related to the regular organization of the collagen molecule in fibrous collagen. When denaturation is induced, the molecule looses its structure and, consequently, the signal intensity decreases. On the contrary, a DP plot makes it possible to monitor tissue structure even when complete disorganization is induced in the tissue. This fact is very important in studying the healing process of strongly denatured tissues, as in the case of burns or accidentally heated areas. Furthermore, a DP plot is not relative to the fibrillar collagen contribution alone, but highlights the conformational modifications of the whole tissue. The use of DP in conjunction to DFT allowed to label each phase transition. For example the 53°C and 66°C images have similar DP values (see Fig. 2), but the DFT spatial distribution is clearly different (see Fig. 1), permitting thus to distinguish between the two temperature points.

#83788 - $15.00 USD Received 4 Jun 2007; revised 25 Jul 2007; accepted 25 Jul 2007; published 21 Aug 2007

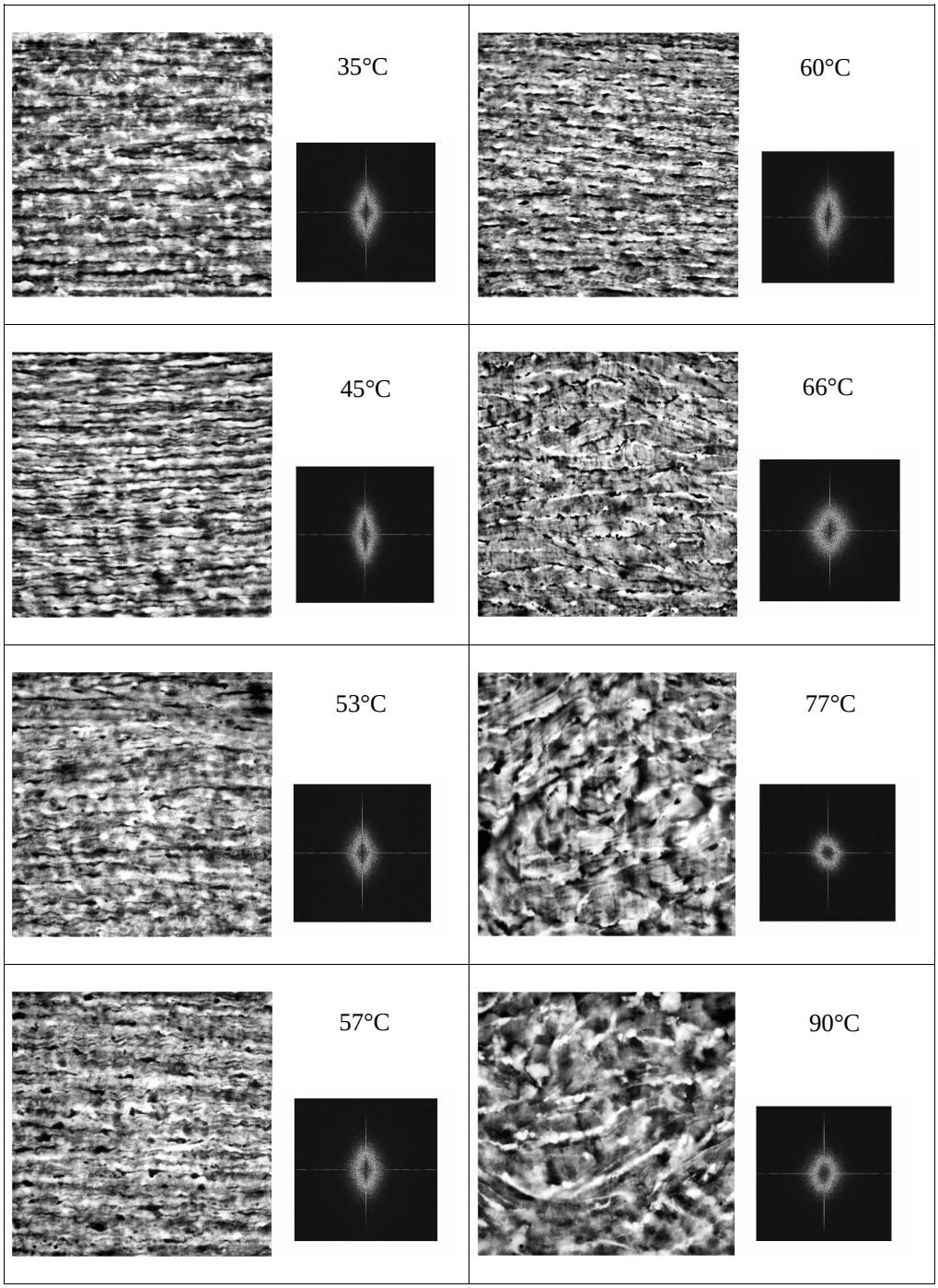

Fig. 1. Fluorescence micro-images of cornea samples heated in a water-bath at different temperatures. The logarithm of the absolute value of the DFT is also shown to the right of each image. The images correspond to an area of 400x400 μm.

#83788 - $15.00 USD Received 4 Jun 2007; revised 25 Jul 2007; accepted 25 Jul 2007; published 21 Aug 2007

The method described here could be proposed as a control system, especially in those surgical procedures in which ICG staining of the tissue is also part of the treatment protocol. For example, it could be used in laser welding of the cornea: this surgical technique is currently performed as a substitute for or support to conventional suturing [23]. Corneal tissue fusion is accomplished after staining the wound edges with an ICG solution, which acts as a photo-enhancing chromophore, and then irradiating with a low-power diode laser emitting at 810 nm. In this case, the simple method that we have set up could be useful in monitoring the photothermal effect induced in corneal tissue. Its extension to *in vivo* real-time applications could be carried out by means of an association with confocal microscopy.

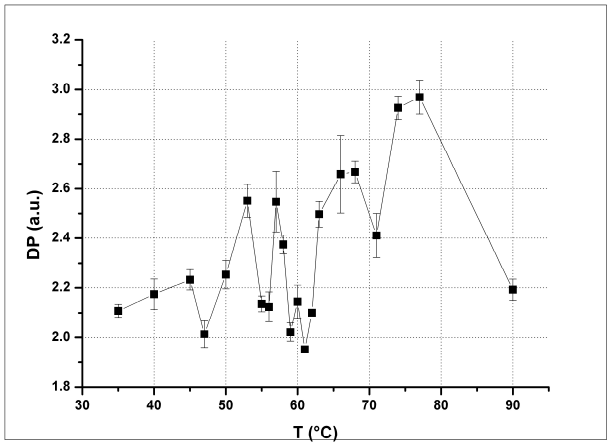

Fig. 2. Plot of the Disorganization Parameter (DP) vs. temperature. Peaks are in correspondence with the principal phase transition temperatures of corneal tissue [5, 16].

5. Conclusion

We have described a procedure for characterizing phase transitions in corneal tissue with the use of a low cost apparatus and the simple implementation of an image-processing algorithm. The system has been found to be extremely precise in detecting thermally-induced morphological modifications in the corneal stroma. It could, therefore, be used as the basis for a control methodology during surgical procedures based on heating treatments in connective tissues.

#83788 - $15.00 USD Received 4 Jun 2007; revised 25 Jul 2007; accepted 25 Jul 2007; published 21 Aug 2007